PRAMANA — journal of physics
© Indian Academy of Sciences
Vol. 54, No. 1
January 2000
pp. 185–201

Variables for probing neutrino oscillation at super-Kamiokande and the Sudbury Neutrino Observatory

DEBASISH MAJUMDAR
Department of Physics, University of Calcutta, 92 Acharya Prafulla Chandra Road, Calcutta 700 009, India

Abstract. We propose several new variables, insensitive to the absolute flux of the incident solar or supernova neutrino beam, which probe the shape of the observed spectrum at super-Kamiokande and Sudbury Neutrino Observatory experiments and can sensitively signal neutrino oscillations. One class of such variables involve moments of the distributions recorded at the two facilities while another variable, specific to SNO, utilises the integrated charged and neutral current signals. The utility of these variables in the context of supernova neutrinos both from the collapse epoch and the post-bounce era is also discussed.

Keywords. Neutrino oscillation.

PACS Nos 14.60.Pq; 26.65.+t

1. Introduction

Recent atmospheric neutrino data [1] from super-Kamiokande neutrino detector (SK) [2] supports a non-zero neutrino mass and oscillation. The huge fiducial volume of the super-Kamiokande detector has already enabled the accumulation of solar neutrino data [3]. Another detector of comparable size, the Sudbury Neutrino Observatory (SNO) [4] is shortly expected to be operational. The latter experiment, because of its capability to detect neutrinos *via* both charged current (CC) as well as neutral current (NC) detection channels, will shed light on the nature of the other neutrino – sequential or sterile. The large data from these two experiments will provide an opportunity to examine signals for neutrino oscillation in different ways.

An uncertainty in drawing conclusions from the neutrino data creeps in through the imperfect knowledge of the incident neutrino flux. For example for the solar case though the shape of the neutrino spectra from the $p - p$ chain, CNO cycle, etc. are known precisely from weak interactions and nuclear physics, their relative and absolute normalizations depend on the physics and astrophysics within the sun and vary from one solar model to another [5]. The boron neutrinos – only which are seen at SK and SNO – are particularly sensitive to the variation of the solar core temperature. It is therefore of importance to formulate methods for the purpose of extracting oscillation information from the observed data in a way such that they are independent of absolute normalization of the initial flux.

Here we examine in detail several variables which depend on (a) moments of distributions seen at SK and SNO and (b) on the ratios of the charged and neutral current signals at SNO in the context of solar neutrinos [6] and supernova neutrinos from both collapse and post bounce phases. These variables are sensitive to the shape of the neutrino spectrum but they are independent of its absolute normalization.

The high statistics data from the new detectors make such a study feasible. We illustrate how our proposed variables yield direct information on the neutrino mixing angles and mass splittings. We show how the variables can further be used to distinguish whether the ν_e oscillates to a sequential neutrino or to a sterile one. Some similar ideas have also been advocated in ref. [7,8] where the focus has been on the energy spectrum of the scattered electron neutrino at SNO, the MSW mechanism etc. In this work, we restrict ourselves to two flavour vacuum oscillations. A detailed analysis of actual solar neutrino data given in [3] using these variables for both vacuum and MSW cases are in progress [9].

Neutrinos are emitted from two distinct epochs of a supernova explosion. In the collapse phase, only ν_e produced from electron capture on free protons and heavy nuclei, are emitted while in the post-bounce era neutrinos of all three flavours (and their antiparticles) are produced. While the detection of the latter for a supernova within a 10 kpc distance is very likely, those from the former will be observable only if the explosion occurs within a distance of about 1 kpc. Some initial results on these issues have been reported earlier [10].

In the next section we introduce the variables which we propose for probing oscillations of solar and supernova neutrinos to sequential or sterile ones. In §3 we give the results of our analysis. We end in §4 with some discussions.

2. The variables

We introduce in this section variables insensitive to the absolute normalization of the incident flux which may be used as diagnostic tools for solar and supernova neutrino oscillations at super-Kamiokande and SNO. We restrict ourselves to the two-flavour vacuum oscillation case.

2.1 *Neutrino oscillations at super-Kamiokande and SNO*

In the two-flavour case, the probability of an electron neutrino of energy E_ν to oscillate to a neutrino of a different type, ν_x, after the traversal of a distance L is

$$P_{\nu_e\to\nu_x} = \sin^2(2\vartheta)\sin^2\left(\frac{\pi L}{\lambda}\right), \tag{1}$$

where ϑ is the mixing angle. λ is the oscillation length given, in terms of the mass-squared difference Δ, by

$$\lambda = 2.47\left(\frac{E_\nu}{\mathrm{MeV}}\right)\left(\frac{\mathrm{eV}^2}{\Delta}\right)\ \mathrm{m}\,. \tag{2}$$

From probability conservation: $P_{\nu_e\to\nu_e} = 1 - P_{\nu_e\to\nu_x}$.

In the above ν_x can either be a sequential neutrino, ν_μ or ν_τ, or a sterile neutrino, ν_s. At super-Kamiokande the neutrinos are detected via $\nu - e$ scattering. An electron neutrino is detected through both charged current (CC) and neutral current (NC) weak interactions. For ν_μ or ν_τ the detection is through NC interaction only. As the sterile neutrino has no such interactions with the detector fluid it will pass unaffected. Therefore for oscillation to a sequential neutrino SK will detect it via NC interaction while for oscillation to a sterile one, the neutrino will not be detected at all. At SNO the electron neutrinos will be detected through (a) CC interactions as well as (b) NC interactions. If oscillations to sequential neutrinos occur then the signal in (a) will be appropriately reduced while that in (b) will remain unaffected. On the other hand if the ν_e oscillates to a sterile state then both the CC and NC signals will suffer depletions.

At this juncture, one point needs attention. The above discussion holds good for solar neutrinos and neutrinos from collapse phase of a supernova as both are electron type neutrinos. But as stated earlier, neutrinos are emitted from a supernova in two stages; one during the collpase stage when only electron type neutrinos are emitted due to the process of electron capture on free protons and heavy nuclei and then during the post core bounce stage when neutrinos of all three flavours (e, μ and τ) and their antineutrinos are emitted. Therefore for discussing oscillation for post core bounce neutrinos in the present framework, one has to consider the consequences of two flavour oscillations for all three types of neutrinos and their antineutrinos.

2.2 *The variables M_n and r_n*

We propose first a set of variables M_n for the extraction of oscillation signals. These variables are the normalized n-th moments of the neutrino distributions under consideration observed at SK and SNO. Specifically,

$$M_n = \frac{\int N_i(E) E^n \mathrm{d}E}{\int N_i(E) \mathrm{d}E}, \tag{3}$$

where i stands for SK or SNO. It is seen from the definition that the uncertainty in the overall normalization of the incident neutrino flux cancels out from M_n.

If neutrino oscillations are operative then we have for solar or collapse phase supernova neutrinos,

$$\begin{aligned} N_{\mathrm{SK}}(E) = \epsilon_{\mathrm{SK}} f(E) \{ & P_{\nu_e \to \nu_e}(E, \Delta, \vartheta) \sigma^e_{\mathrm{SK}}(E) \\ & + P_{\nu_e \to \nu_\mu}(E, \Delta, \vartheta) \sigma^\mu_{\mathrm{SK}}(E) \} N^0_{\mathrm{SK}} \end{aligned} \tag{4}$$

for oscillation to a sequential neutrino indicated by ν_μ in the above. Here, $f(E)$ stands for the incident boron–neutrino fluence or collapse phase supernova neutrino fluence as the case may be, ϵ_{SK} for the detection efficiency which, for the sake of simplicity, is assumed to be energy independent, and N^0_{SK} for the number of electrons in the SK detector of which the neutrinos may scatter. $\sigma^e_{\mathrm{SK}}(E)$ is the ν_e scattering cross-section with both NC and CC contributions whereas $\sigma^\mu_{\mathrm{SK}}(E)$ is the ν_μ cross-section obtained from the NC interaction alone.

If the oscillation is to a sterile neutrino then eq. (4) will be replaced by

$$N_{\rm SK}(E) = \epsilon_{\rm SK} f(E) P_{\nu_e \to \nu_e}(E, \Delta, \vartheta) \sigma^e_{\rm SK}(E) N^0_{\rm SK}. \tag{5}$$

The super-Kamiokande detector uses 32 ktons of light water (H_2O) in which electrons scattered by ν_e are detected via Čerenkov radiation. The $\nu_e - e^-$ scattering cross-section is $\sigma^e_{\rm SK} = 9.4 \times 10^{-44}$ cm$^2(E_\nu/10\ {\rm MeV})$ [11]. The neutral current $\nu_\mu - e^-$ scattering cross-section is $\sigma^\mu_{\rm SK} = 1.6 \times 10^{-44}$ cm$^2(E_\nu/10\ {\rm MeV})$ [11].

Only the CC contributions are relevant at SNO for the determination of the spectrum and we get

$$N^{\rm c.c.}_{\rm SNO}(E) = \epsilon^{\rm c.c.}_{\rm SNO} f(E) P_{\nu_e \to \nu_e}(E, \Delta, \vartheta) \sigma^{\rm c.c.}_{\rm SNO}(E) N^0_{\rm SNO}. \tag{6}$$

$N^0_{\rm SNO}$ is the number of deuteron nuclei in the SNO detector and $\epsilon^{\rm c.c.}_{\rm SNO}$ represents the CC detection efficiency assumed to be independent of the energy. The above result is valid for oscillation to sequential as well as sterile neutrinos since neither of them can interact via the charged current.

The SNO detector has 1 kton of D_2O and neutrinos are primarily detected through the charged and neutral current disintegration of the deuteron: $\nu_e + d \to e^- + p + p$, $\nu + d \to \nu + p + n$, respectively. The e^- in the CC reaction is identified through its Čerenkov radiation. The neutral current detection is calorimetric and only the integrated signal is measured through this channel. Therefore, shape of the signal is measured via the charged current interaction. For the cross-section for this process we use $\sigma^{\rm c.c.}_{\rm SNO} = 1.7 \times 10^{-44} {\rm cm}^2 (E_\nu - 1.44)^{2.3}$ [12].

Unlike for solar and collapse phase neutrinos which are only electron type, several new things are to be taken into consideration for detection of post bounce neutrinos as they are of six varieties (neutrinos of three flavours and their antineutrinos, namely, the ν_e, the $\bar{\nu}_e$ and the ν_x where the latter stands for neutrinos as well as anti-neutrinos of the μ and τ types). For the present analysis we use the spectra for all those six types of neutrinos, extracted from the results presented in [13]. Oscillations of those six neutrinos will therefore give rise to a complicated scenario [14]. We restrict ourselves, as earlier, to two flavour vacuum neutrino oscillations. Thus, for example, if we consider $\nu_e \leftrightarrow \nu_\mu$ oscillations, then the ν_τ neutrinos and anti-neutrinos will be entirely unaffected while both neutrinos and anti-neutrinos of the electron and muon type undergo oscillations.

If we indicate the initial fluence of ν_e, $\bar{\nu}_e$ and the neutrinos (and the antineutrinos) of the μ and τ flavours by $f^e(E)$, $\bar{f}^e(E)$ and $f^x(E)$ respectively then the observed signal at SK can be written as

$$\begin{aligned} N_{\rm SK}(E) = \epsilon_{\rm SK} N^0_{\rm SK} & \\ \times \Big[& \left\{ f^e(E) P_{\nu_e \to \nu_e}(E,\Delta,\vartheta) + f^x(E) P_{\nu_\mu \to \nu_e}(E,\Delta,\vartheta) \right\} \sigma^e_{\rm SK}(E) \\ & + \left\{ f^e(E) P_{\nu_e \to \nu_\mu}(E,\Delta,\vartheta) + f^x(E) P_{\nu_\mu \to \nu_\mu}(E,\Delta,\vartheta) + f^x(E) \right\} \sigma^\mu_{\rm SK}(E) \\ & + \left\{ \bar{f}^e(E) P_{\nu_e \to \nu_e}(E,\Delta,\vartheta) + f^x(E) P_{\nu_\mu \to \nu_e}(E,\Delta,\vartheta) \right\} \bar{\sigma}^e_{\rm SK}(E) \\ & + \left\{ \bar{f}^e(E) P_{\nu_e \to \nu_\mu}(E,\Delta,\vartheta) + f^x(E) P_{\nu_\mu \to \nu_\mu}(E,\Delta,\vartheta) + f^x(E) \right\} \bar{\sigma}^\mu_{\rm SK}(E) \Big] \end{aligned} \tag{7}$$

for oscillation to a sequential neutrino indicated by ν_μ in the above. Here $\bar{\sigma}^x_{\rm SK}(E)$ is the $\bar{\nu}_\mu$ or $\bar{\nu}_\tau$ scattering cross-section of electrons which proceeds via the neutral current and is 1.3×10^{-44} cm$^2 p_e E_e/$(10 MeV). For the $\bar{\nu}_e$, there is a charged current contribution so that the total $\bar{\nu}_e - e$ scattering cross-section is $3.9 \times 10^{-44} {\rm cm}^2\, E/(10\,{\rm MeV})$. $\bar{\sigma}^e_{\rm SK}(E)$

receives an additional (dominant) contribution from the process $\bar{\nu}_e + p \to e^+ + n$ which is $9.4 \times 10^{-42}\mathrm{cm}^2\, p_e E_e/(10\,\mathrm{MeV})^2$ where p_e is the electron momentum and $E_e = E - 1.3$ MeV its energy [11].

If instead, oscillations to a sterile neutrino are operative, then eq. (7) will be replaced by

$$N_{\mathrm{SK}}(E) = [f^e(E)P_{\nu_e\to\nu_e}(E,\Delta,\vartheta)\sigma^e_{\mathrm{SK}}(E) + 2f^x(E)\sigma^\mu_{\mathrm{SK}}(E) + \bar{f}^e(E)P_{\nu_e\to\nu_e}(E,\Delta,\vartheta)\bar{\sigma}^e_{\mathrm{SK}}(E) + 2f^x(E)\bar{\sigma}^x_{\mathrm{SK}}(E)]\,\epsilon_{\mathrm{SK}}N^0_{\mathrm{SK}} \tag{8}$$

Only the CC contributions are relevant at SNO for the extraction of the spectral shape and in this case the relevant formula valid for oscillation to a sequential state is

$$N^{\mathrm{c.c.}}_{\mathrm{SNO}}(E) = \epsilon^{\mathrm{c.c.}}_{\mathrm{SNO}}N^0_{\mathrm{SNO}} \times \left[\left\{f^e(E)P_{\nu_e\to\nu_e}(E,\Delta,\vartheta) + f^x(E)P_{\nu_\mu\to\nu_e}(E,\Delta,\vartheta)\right\}\sigma^{\mathrm{c.c.}}_{\mathrm{SNO}}(E) + \left\{\bar{f}^e(E)P_{\nu_e\to\nu_e}(E,\Delta,\vartheta) + f^x(E)P_{\nu_\mu\to\nu_e}(E,\Delta,\vartheta)\right\}\bar{\sigma}^{\mathrm{c.c.}}_{\mathrm{SNO}}(E)\right] \tag{9}$$

while for oscillation to sterile neutrinos it is

$$N^{\mathrm{c.c.}}_{\mathrm{SNO}}(E) = [f^e(E)P_{\nu_e\to\nu_e}(E,\Delta,\vartheta)\sigma^{\mathrm{c.c.}}_{\mathrm{SNO}}(E) + \bar{f}^e(E)P_{\nu_e\to\nu_e}(E,\Delta,\vartheta)\bar{\sigma}^{\mathrm{c.c.}}_{\mathrm{SNO}}(E)]\,\epsilon^{\mathrm{c.c.}}_{\mathrm{SNO}}N^0_{\mathrm{SNO}}. \tag{10}$$

The variable r_n is defined as ratios of the moments obtained from two experiments namely SK and SNO,

$$r_n = \frac{(M_n)_{\mathrm{SK}}}{(M_n)_{\mathrm{SNO}}}. \tag{11}$$

With high statistics data from both experiments the variables r_n may be taken as indicative of the oscillation parameters.

2.3 *The variable* R_{SNO}

The variable R_{SNO} is defined as the ratio of the total signal in the NC channel, $\int N^{\mathrm{n.c.}}_{\mathrm{SNO}}$, to the total (energy integrated) signal in the CC channel, $\int N^{\mathrm{c.c.}}_{\mathrm{SNO}}$ and it is a good probe for oscillations. Thus

$$R_{\mathrm{SNO}} = \frac{\int N^{\mathrm{n.c.}}_{\mathrm{SNO}}}{\int N^{\mathrm{c.c.}}_{\mathrm{SNO}}}. \tag{12}$$

For oscillation to a sequential neutrino for solar or collapse phase supernova case,

$$\int N^{\mathrm{n.c.}}_{\mathrm{SNO}} = \int \epsilon^{\mathrm{n.c.}}_{\mathrm{SNO}} f(E)\sigma^{\mathrm{n.c.}}_{\mathrm{SNO}}(E)N^0_{\mathrm{SNO}}\mathrm{d}E \tag{13}$$

in which $\epsilon^{\mathrm{n.c.}}_{\mathrm{SNO}}$ is the detection efficiency for the NC channel and

$$\int N^{\rm c.c.}_{\rm SNO} = \int \epsilon^{\rm c.c.}_{\rm SNO} f(E) P_{\nu_e\to\nu_e}(E,\Delta,\vartheta)\sigma^{\rm c.c.}_{\rm SNO}(E) N^0_{\rm SNO}{\rm d}E. \tag{14}$$

It is obvious that $R_{\rm SNO}$ is independent of the absolute normalization of the incident neutrino flux $f(E)$ and only depends on its shape.

If oscillations to sterile neutrinos take place then eq. (13) is replaced by

$$\int N^{\rm n.c.}_{\rm SNO} = \int \epsilon^{\rm n.c.}_{\rm SNO} f(E) P_{\nu_e\to\nu_e}(E,\Delta,\vartheta)\sigma^{\rm n.c.}_{\rm SNO}(E) N^0_{\rm SNO}{\rm d}E \tag{15}$$

and eq. (14) remains unchanged.

For the NC cross-section $\sigma^{\rm n.c.}_{\rm SNO}$ we use $0.85\times 10^{-44}{\rm cm}^2(E_\nu - 2.2)^{2.3}$ [12]. For simplicity, we have assumed $\epsilon^{\rm n.c.}_{\rm SNO}$ to be independent of the energy and further equal to the efficiency of the CC reaction $\epsilon^{\rm c.c.}_{\rm SNO}$. If instead, $\epsilon^{\rm n.c.}_{\rm SNO}/\epsilon^{\rm c.c.}_{\rm SNO} = r_\epsilon$ and it can be taken to be independent of the energy to a good approximation, then our results for $R_{\rm SNO}$ will be multiplied by this factor.

For post-bounce epoch neutrinos the ratio, $R_{\rm SNO}$, unlike the case of solar or collapse phase, is sensitive to oscillations of an electron neutrino to a sterile state. As before

$$R_{\rm SNO} = \frac{\int N^{\rm n.c.}_{\rm SNO}}{\int N^{\rm c.c.}_{\rm SNO}}, \tag{16}$$

where for oscillation to a sequential neutrino

$$\int N^{\rm n.c.}_{\rm SNO} = \int \left[\{f^e(E) + 2f^x(E)\}\,\sigma^{\rm n.c.}_{\rm SNO}(E) + \left\{\bar{f}^e(E) + 2f^x(E)\right\}\bar{\sigma}^{\rm n.c.}_{\rm SNO}(E)\right]\epsilon^{\rm n.c.}_{\rm SNO} N^0_{\rm SNO}{\rm d}E, \tag{17}$$

where $\bar{\sigma}^{\rm n.c.}_{\rm SNO}(E) = \sigma^{\rm n.c.}_{\rm SNO}(E)$, while for the sterile neutrino alternative

$$\int N^{\rm n.c.}_{\rm SNO} = \int \left[\{f^e(E)P_{\nu_e\to\nu_e}(E,\Delta,\vartheta) + 2f^x(E)\}\,\sigma^{\rm n.c.}_{\rm SNO}(E) + \left\{\bar{f}^e(E)P_{\nu_e\to\nu_e}(E,\Delta,\vartheta) + 2f^x(E)\right\}\bar{\sigma}^{\rm n.c.}_{\rm SNO}(E)\right]\epsilon^{\rm n.c.}_{\rm SNO} N^0_{\rm SNO}{\rm d}E \tag{18}$$

and

$$\int N^{\rm c.c.}_{\rm SNO} = \int N^{\rm c.c.}_{\rm SNO}(E){\rm d}E, \tag{19}$$

where $N^{\rm c.c.}_{\rm SNO}(E)$ is given by eq. (9) or eq. (10) depending on whether oscillation of electron neutrinos takes place to sequential or sterile neutrinos, respectively.

3. Results

3.1 *Solar case*

Some results for M_1 and M_2 for solar neutrinos are presented in table 1 for different values of the mass splitting Δ and the mixing angle ϑ. Note that at SNO, these variables cannot distinguish between the sequential and sterile neutrino alternatives. It is seen from table 1 that at super-Kamiokande for the smaller mixing angle ($\vartheta = 30\,^\circ$) for any Δ the difference between the values of M_1 (as well as M_2) for the sequential and sterile neutrino cases does not exceed 5% but the variation from the no oscillation ($\Delta = 0$) limit can be as large as 10%. It is seen from the table that for $\vartheta = 45°$, the ranges of variation of M_1 and M_2 are significantly larger and a distinction between the sequential and sterile alternatives ought to be possible. At SNO, M_1 and M_2 vary over larger ranges and, in particular at $\Delta = 0.6 \times 10^{-10}$ eV^2 and $\vartheta = 45°$, it is as much as 15% for M_1 and 20% for M_2.

In figure 1 we present the contours of constant M_1 in the $\Delta - \vartheta$ plane for (a) SK sequential, (b) SK sterile and (c) SNO cases. Using these contours, one may readily get the values of Δ and ϑ if M_1 is measured precisely. It can also be seen from figure 1 that around $\Delta = 0.6 \times 10^{-10}$ eV^2 and $\vartheta = 45°$, M_1 changes rather sharply. A detailed analysis for the variable r_n is done in our work [15].

In order to study the variable $R_{\rm SNO}$, we have calculated its value for different choices of ϑ and Δ. In table 2, we present the results for three choices of the mixing angle

Table 1. M_1 and M_2 for solar neutrinos for different values of the mass splitting Δ for the super-Kamiokande and SNO detectors. For the former, results are presented for oscillation to sequential as well as sterile neutrinos. For SNO the two cases yield the same value of M_n. Two choices of the mixing angle $\vartheta = 30°$ and $45°$ have been considered.

Δ in 10^{-10} eV^2	M_1						M_2					
	$\vartheta = 30°$			$\vartheta = 45°$			$\vartheta = 30°$			$\vartheta = 45°$		
	SK		SNO	SK		SNO	SK		SNO	SK		SNO
	seq.	st.		seq.	st.		seq.	st.		seq.	st.	
0.0	8.49	8.49	9.35	8.49	8.49	9.35	76.3	76.3	91.4	76.3	76.3	91.4
0.3	8.76	8.83	9.62	8.89	9.03	9.76	80.8	82.1	96.3	83.0	85.3	98.8
0.6	8.73	8.87	9.81	9.01	9.77	10.67	80.9	83.6	100.5	86.31	101.0	117.5
0.9	7.85	7.57	8.52	7.34	6.57	7.09	65.7	61.2	77.4	57.4	44.8	53.1
1.2	8.13	8.02	8.67	7.94	7.74	8.21	69.3	67.2	78.4	65.7	61.9	69.4
1.5	8.71	8.78	9.36	8.82	8.93	9.37	79.2	80.0	90.6	80.6	82.0	90.1
1.8	8.79	8.88	9.75	8.94	9.10	9.95	81.8	83.5	98.6	84.6	87.5	102.2
2.1	8.66	8.71	9.76	8.75	8.85	10.02	80.0	81.2	100.1	82.1	84.5	105.5
2.4	8.47	8.46	9.45	8.46	8.44	9.52	76.3	76.3	94.4	76.3	76.4	96.7
2.7	8.26	8.18	9.02	8.12	7.95	8.74	72.2	70.7	85.6	69.6	66.6	80.8
3.0	8.34	8.29	8.99	8.25	8.15	8.72	73.1	72.0	84.1	71.3	69.1	78.6
3.5	8.54	8.56	9.37	8.57	8.59	9.38	77.0	77.2	91.2	77.4	77.8	91.1
4.0	8.61	8.65	9.56	8.67	8.75	9.69	78.6	79.3	95.8	79.9	81.3	98.5
4.5	8.45	8.44	9.35	8.43	8.40	9.36	75.8	75.6	92.1	75.4	75.1	92.5
5.0	8.45	8.44	9.23	8.43	8.41	9.14	75.4	75.1	88.9	74.8	74.2	87.1
5.5	8.48	8.47	9.29	8.47	8.46	9.26	75.9	75.8	90.1	75.7	75.4	89.2
6.0	8.53	8.54	9.41	8.55	8.57	9.46	77.0	77.3	92.8	77.4	77.9	93.7

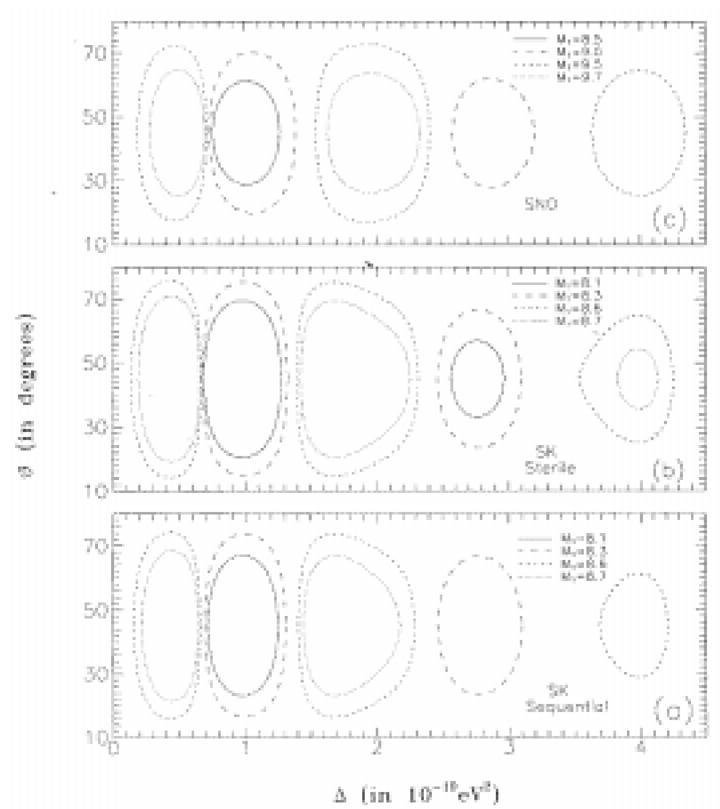

Figure 1. Contours of constant M_1 for solar neutrinos in the Δ–ϑ plane. For the case of SNO, both the sequential and sterile scenarios give identical results.

$\vartheta = 15°, \quad 30°$ and $45°$. In the absence of oscillations we find $R_{\rm SNO}$ = 0.382. A significantly different $R_{\rm SNO}$ from its no-oscillation limit will be a clear indication of oscillation to a sequential neutrino. In particular, for $\Delta = 0.6 \times 10^{-10}$ eV^2 and $\vartheta = 45°$, $R_{\rm SNO}$ will be as high as 2.1 for oscillation to sequential neutrinos. A more elaborate discussion on this and the contours of constant $R_{\rm SNO}$ in the $\Delta - \vartheta$ plane for oscillation to sequential neutrinos are given in [6,15].

3.2 *Supernova collapse phase*

The collapse phase neutrino spectra from a realistic range of nuclear physics inputs as well as several stellar masses on the main sequence are presented in refs [16,17]. In the present work we use the neutrino spectrum of a $15M_\odot$ star as presented there and choose the distance of the supernova to be 1 kpc. If the supernova is much further away then the flux of neutrinos will be too weak to be detected with significant statistics.

For this case, M_1 and M_2 for different values of Δ are presented in table 3 for maximal mixing ($\vartheta = 45°$). Results for oscillation to sequential and sterile neutrinos are separately

Table 2. $R_{\rm SNO}$ for solar neutrinos for different values of the mixing angle, ϑ, and the mass splitting, Δ.

Δ in 10^{-10} eV^2	$R_{\rm SNO}$					
	$\vartheta = 15^\circ$		$\vartheta = 30^\circ$		$\vartheta = 45^\circ$	
	Sequential	Sterile	Sequential	Sterile	Sequential	Sterile
0.0	0.382	0.382	0.382	0.382	0.382	0.382
0.3	0.422	0.384	0.532	0.389	0.613	0.392
0.6	0.480	0.383	0.991	0.387	2.117	0.396
0.9	0.467	0.378	0.848	0.362	1.428	0.337
1.2	0.438	0.380	0.623	0.375	0.788	0.370
1.5	0.422	0.383	0.537	0.387	0.620	0.390
1.8	0.417	0.383	0.512	0.386	0.577	0.388
2.1	0.431	0.383	0.582	0.387	0.706	0.390
2.4	0.444	0.382	0.660	0.383	0.873	0.384
2.7	0.444	0.380	0.658	0.375	0.867	0.370
3.0	0.444	0.381	0.659	0.379	0.869	0.377
3.5	0.431	0.382	0.582	0.381	0.705	0.380
4.0	0.434	0.383	0.597	0.386	0.735	0.388
4.5	0.435	0.382	0.606	0.381	0.753	0.380
5.0	0.440	0.382	0.634	0.381	0.813	0.381
5.5	0.437	0.382	0.614	0.381	0.770	0.381
6.0	0.434	0.382	0.597	0.382	0.735	0.382

Table 3. M_1, and M_2 for supernova collapse phase neutrinos for different values of the mass splitting Δ for the SK and SNO detectors. For SNO, the two cases yield the same value of M_n. The ratios r_1 and r_2 are also presented. The mixing angle ϑ has been chosen to be 45°.

Δ in 10^{-18} eV^2	M_1			r_1		M_2			r_2	
	SK		SNO	seq.	st.	SK		SNO	seq.	st.
	seq.	st.				seq.	st.			
0.0	13.3	13.3	16.1	0.83	0.83	202.4	202.4	281.7	0.72	0.72
0.6	11.3	9.9	13.9	0.81	0.71	152.3	120.6	234.0	0.65	0.52
1.2	13.5	13.6	15.6	0.87	0.87	203.1	203.3	256.5	0.79	0.79
1.8	13.9	14.2	17.5	0.79	0.81	223.9	232.3	328.8	0.68	0.71
2.4	12.7	12.4	14.9	0.85	0.83	182.0	172.9	243.2	0.75	0.71
3.0	13.5	13.5	16.0	0.84	0.84	204.2	205.0	272.8	0.75	0.75
4.0	13.3	13.3	16.1	0.83	0.83	201.1	200.1	284.6	0.71	0.70
5.0	13.4	13.4	16.1	0.83	0.83	203.3	203.7	280.3	0.73	0.73
6.0	13.3	13.3	16.2	0.82	0.82	202.1	201.9	283.5	0.71	0.71

presented for SK. The SNO CC signal does not distinguish between these alternatives. The ratios r_1 and r_2 (see eq. (11)) are also presented in table 3. It is seen from this table that the variation in M_1 can be 15% at both SK and SNO for some values of the oscillation parameters while for M_2 it can be as large as 40% (25%) at SNO (SK). At SK, the variation is larger in the sterile neutrino scenario.

Unlike the solar neutrino case, here, even the shape of the incident neutrino spectrum is not precisely known. In order to assess that whether the uncertainty in initial flux can mimic the effect due to oscillation, we estimate the uncertainties considering the situations in one case, the electron capture only on free protons while in the other, electron capture exclusively on heavy nuclei. Further, we estimate the uncertainties due to the unknown mass of the progenitor by considering a $15M_\odot$ and a $25M_\odot$ star. The results are presented in table 4. We found that the uncertainties in M_1 and M_2 are larger than that due to oscillations which were presented in table 3. Thus, for the collapse phase neutrinos, M_1 and M_2 cannot be used with full confidence for probing neutrino oscillations. The situation is somewhat better with the variables r_1 and r_2 in the sense that variation due to uncertainties in the initial spectrum can be at most 0.83 – 0.91 and 0.72 – 0.84 respectively and cannot mask an effect due to oscillations at least for some ranges of the mixing parameters. In figure 2, we present r_1, r_2, and r_3 as a function of Δ for two values of the mixing angle ϑ. One sees from figure 2 that around $\Delta = 1 \times 10^{-18}$ eV^2 these variables can clearly distinguish between oscillation to a sequential or to a sterile neutrino for $\vartheta = 45°$.

A better variable for the purpose turns out to be R_{SNO}. The variation of R_{SNO} with the mass splitting Δ is shown in table 5 where the mixing angle has been chosen to be $\vartheta = 45°$. From these results it is seen that R_{SNO} can be increased several times if oscillation to sequential neutrinos occur and can achieve values as high as 1.7. We have done a detailed study of this variable for collapse phase neutrinos and the results are presented in [10].

3.3 *Supernova post bounce phase*

Some results for M_1, M_2 and r_1, r_2 for post-bounce epoch neutrinos are presented in table 6 for different values of the mass splitting Δ for the mixing angle $\vartheta = 45°$. Note that for

Table 4. M_1, M_2, r_1, and r_2 in the absence of oscillations for collapse phase neutrino spectra obtained by changing the parameters for the progenitor star.

Progenitor Spectrum	$15M_\odot$						$25M_\odot$					
	M_1		r_1	M_2		r_2	M_1		r_1	M_2		r_2
	SK	SNO		SK	SNO		SK	SNO		SK	SNO	
Combined	13.3	16.1	0.83	202	282	0.72	13.3	15.9	0.84	200	275	0.73
Only free protons	15.9	17.5	0.91	270	321	0.84	14.9	16.8	0.89	241	300	0.81
Only heavy nuclei	9.1	10.4	0.87	89	118	0.75	8.9	10.3	0.87	86	115	0.75

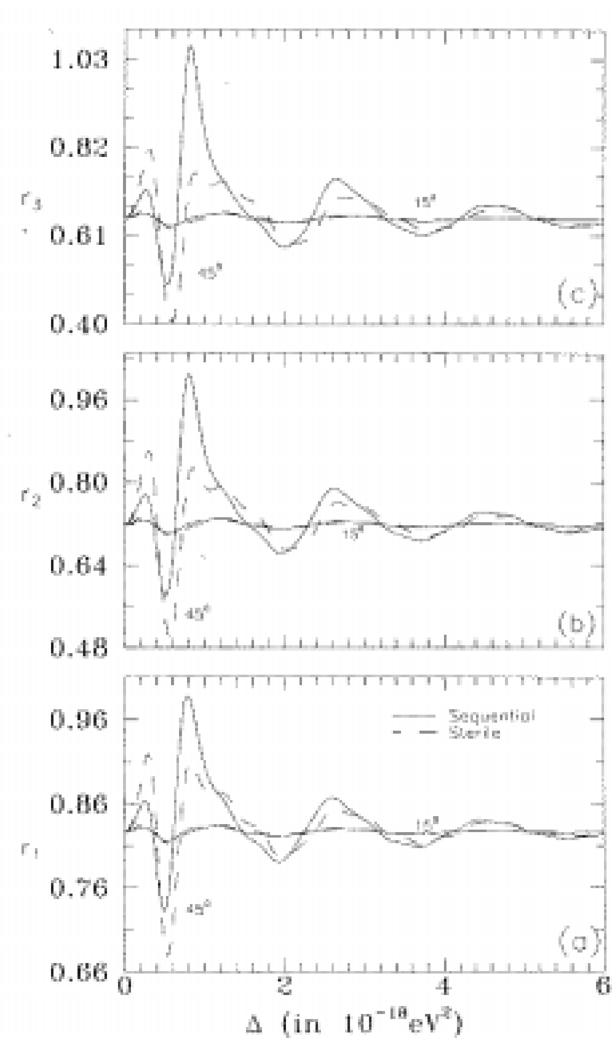

Figure 2. The variables (a) r_1, (b) r_2, and (c) r_3 for supernova collapse phase neutrinos as a function of the mass splitting Δ for two values of the mixing angle ϑ = 45° and 15°.

post-bounce neutrinos, SNO can distinguish between oscillation to sequential and sterile neutrinos. Since the spectra of the electron- and muon-type neutrinos are different, the CC signal changes differently for oscillation to sequential or sterile neutrinos. Due to the higher energy of the ν_μ and ν_τ, oscillation to sequential neutrinos always increases the signal at both SK and SNO while for the sterile case both larger and smaller values are possible depending on Δ. It is seen from table 6 that the effect of oscillations is most pronounced around $\Delta = 1.2 \times 10^{-19}$ eV^2. For example, for the sterile alternative, for M_1 the deviation from the no-oscillation value is about 25% (20%) at SK (SNO), for M_2 it is 45% (39%).

Table 5. $R_{\rm SNO}$ for collapse phase neutrinos as a function of the mass splitting Δ for $\vartheta = 45°$.

Δ in 10^{-18} eV^2	$R_{\rm SNO}$	
	Sequential	Sterile
0.0	0.431	0.431
0.3	0.844	0.441
0.6	1.704	0.419
0.9	1.356	0.419
1.2	0.833	0.431
1.5	0.661	0.434
1.8	0.708	0.434
2.1	0.890	0.433
2.4	1.014	0.427
2.7	0.990	0.427
3.0	0.886	0.430
3.5	0.797	0.433
4.0	0.843	0.431
4.5	0.901	0.430
5.0	0.959	0.434
5.5	0.950	0.435
6.0	0.769	0.430
6.5	0.903	0.432

Table 6. M_1 and M_2 for post-bounce epoch neutrinos for different values of the mass splitting Δ for the SK and SNO detectors. Results are presented for oscillation to sequential as well as sterile neutrinos. r_1 and r_2 are also shown for both cases. The mixing angle ϑ has been chosen to be $45°$.

Δ in 10^{-19} eV^2	M_1				r_1		M_2				r_2	
	SK		SNO		seq.	st.	SK		SNO		seq.	st.
	seq.	st.	seq.	st.			seq.	st.	seq.	st.		
0.0	23.1	23.1	22.5	22.5	1.02	1.02	599.3	599.3	573.0	573.0	1.05	1.05
0.3	24.3	25.4	24.3	24.9	1.00	1.02	650.1	696.6	649.7	673.1	1.00	1.03
0.6	25.0	26.7	25.5	26.2	0.98	1.02	688.8	792.8	712.8	767.7	0.97	1.03
0.9	25.0	20.0	25.9	19.1	0.97	1.05	696.8	504.4	736.2	462.7	0.95	1.09
1.2	25.3	17.2	26.4	16.9	0.96	1.02	708.8	328.2	764.5	315.1	0.93	1.04
1.5	25.5	19.4	26.8	19.1	0.95	1.01	719.8	400.0	786.5	390.4	0.92	1.02
1.8	25.4	21.9	26.6	21.6	0.95	1.02	717.1	518.0	781.9	503.5	0.92	1.03
2.1	25.0	23.8	25.8	23.4	0.97	1.02	696.6	619.2	742.1	598.7	0.94	1.03
2.4	24.5	24.9	24.7	24.3	0.99	1.02	666.8	685.1	682.4	658.3	0.98	1.04
2.7	24.1	25.1	24.0	24.4	1.00	1.03	643.6	708.1	637.9	676.0	1.01	1.05
3.0	24.0	24.6	24.0	23.9	1.00	1.03	638.8	688.9	633.0	654.4	1.01	1.05
3.5	24.6	22.8	25.1	22.2	0.98	1.03	666.8	596.8	690.7	567.2	0.97	1.05
4.0	25.2	21.6	26.2	21.2	0.96	1.02	702.7	521.0	754.2	500.5	0.93	1.04
4.5	25.4	22.0	26.5	21.5	0.96	1.02	714.5	531.2	773.3	512.0	0.92	1.04
5.0	25.0	23.2	25.9	22.6	0.97	1.02	697.4	594.9	742.4	570.7	0.94	1.04
5.5	24.6	24.0	25.0	23.4	0.98	1.03	669.6	647.8	691.3	619.2	0.97	1.05
6.0	24.3	23.8	24.6	23.1	0.99	1.03	653.3	642.9	664.3	612.4	0.98	1.05
6.5	24.4	22.8	24.9	22.2	0.98	1.03	662.4	596.6	684.3	567.5	0.97	1.05
7.0	25.1	23.0	26.0	22.6	0.97	1.02	696.1	587.8	739.8	564.6	0.94	1.04
7.5	25.2	22.3	26.1	21.8	0.96	1.02	703.2	555.3	753.6	532.8	0.93	1.04

In order to estimate the sensitivity of these variables with the change in input spectra of the neutrinos, we consider a variation of $\pm 30\%$ in the absolute normalization of each of $f^e(E)$, $\bar{f}^e(E)$, and $f^x(E)$. It has been found that these variables are remarkably stable [15]. Hence these variables can be powerful tools to probe oscillations.

In figure 3, r_1, r_2, and r_3 are presented as a function of Δ for two values of the mixing angle, $\vartheta = 45°$ and $15°$. The different nature of the sequential and sterile cases – due to the presence of the other sequential neutrinos in the parent beam – is noteworthy.

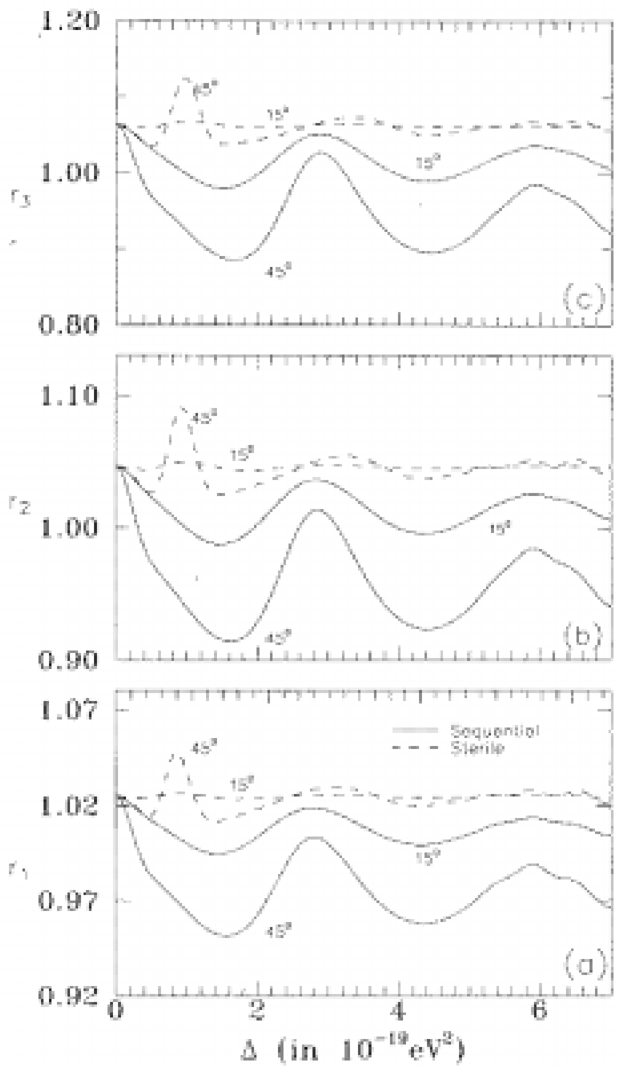

Figure 3. The variables (a) r_1, (b) r_2, and (c) r_3 for supernova post-bounce phase neutrinos as a function of the mass splitting Δ for two values of the mixing angle ϑ = $45°$ and $15°$.

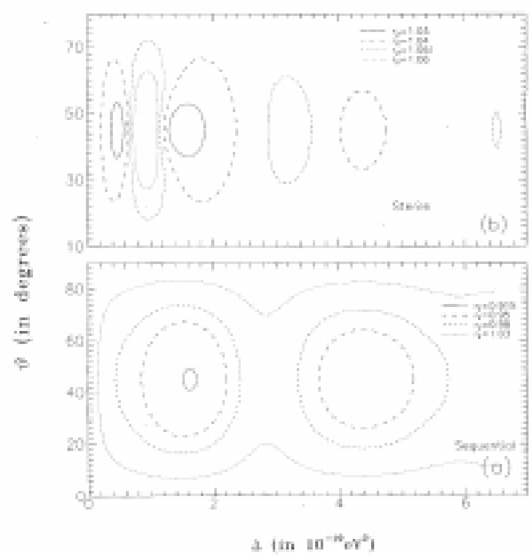

Figure 4. Contours of constant r_2 for supernova post-bounce phase neutrinos in the Δ–ϑ plane.

Table 7. $R_{\rm SNO}$ for post-bounce epoch neutrinos as a function of the mass splitting Δ for $\vartheta = 15^\circ$ and 45°. Results are presented for oscillation to sequential as well as sterile neutrinos.

Δ in 10^{-19} eV^2	$R_{\rm SNO}$			
	$\vartheta = 15^\circ$		$\vartheta = 45^\circ$	
	Sequential	Sterile	Sequential	Sterile
0.0	1.929	1.929	1.929	1.929
0.3	1.952	2.050	2.024	2.584
0.6	1.894	2.212	1.796	4.837
0.9	1.796	2.247	1.488	6.007
1.2	1.749	2.201	1.368	4.565
1.5	1.765	2.145	1.406	3.552
1.8	1.817	2.108	1.549	3.101
2.1	1.876	2.093	1.733	2.945
2.4	1.915	2.094	1.876	2.951
2.7	1.923	2.104	1.908	3.055
3.0	1.905	2.118	1.836	3.211
3.5	1.850	2.139	1.647	3.469
4.0	1.814	2.145	1.539	3.555
4.5	1.818	2.137	1.552	3.444
5.0	1.851	2.125	1.652	3.292
5.5	1.882	2.119	1.753	3.219
6.0	1.881	2.116	1.751	3.186
6.5	1.856	2.118	1.667	3.210
7.0	1.844	2.143	1.628	3.523
7.5	1.830	2.136	1.585	3.430

In figure 4 we present the contours of constant r_2 in the $\Delta - \vartheta$ plane for both the sequential and sterile neutrino cases. For sterile case, we have presented contours for two values of the variable larger than the no-oscillation limit while two are smaller. Note that these contours alternate as a function of Δ which is a reflection of the oscillating behaviour of r_n seen in figure 3. For the sequential case however, all the four values of r_2 are less than the no oscillation limit. Such a choice is also indicated by figure 3.

In table 7, we present the effect of oscillations on $R_{\rm SNO}$ as a function of Δ for $\vartheta = 15^\circ$ and 45°. It is evident that $R_{\rm SNO}$ varies over a wide range in the sterile neutrino alternative while for the case of sequential neutrino, this variation is much less. In figure 5 contours of constant $R_{\rm SNO}$ in $\Delta - \theta$ plane for oscillation to sterile neutrinos are presented. For a more detailed analysis of this variable see our work in [15].

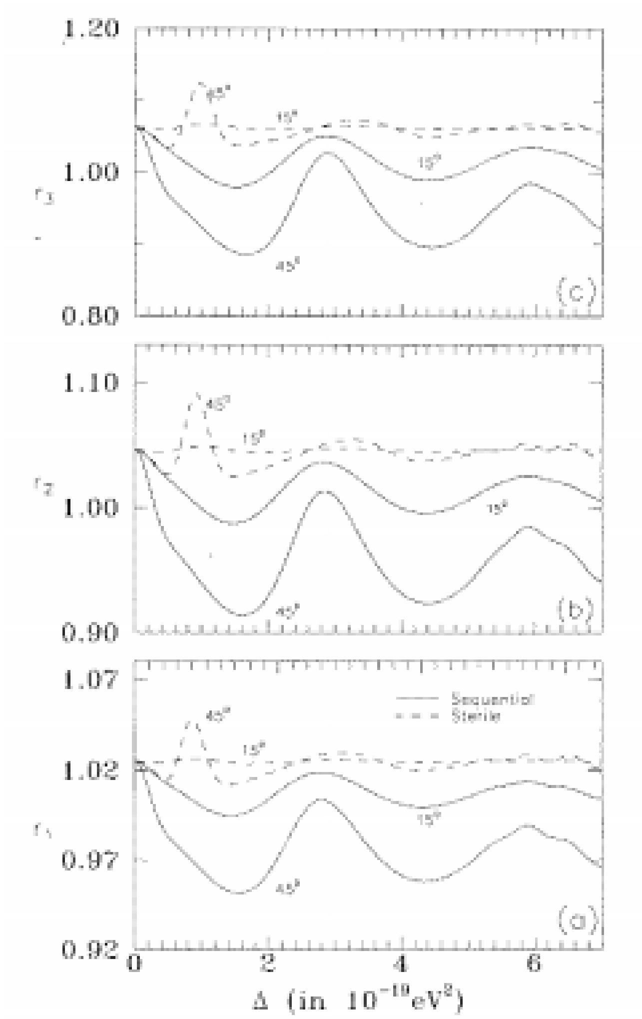

Figure 5. Contours of constant $R_{\rm SNO}$ in the Δ–ϑ plane for oscillation of post-bounce phase neutrinos to sterile neutrinos.

4. Discussions and conclusions

The variables that we have discussed can be powerful diagnostic tools to search for neutrino oscillations in solar and supernova neutrino data obtained at SK and SNO. The effectiveness of the variables lies in the fact that they are simple in nature and more importantly they do not depend on the absolute normalization of initial flux. Though, in this work, we have illustrated their utility to signal two flavour vacuum neutrino oscillations only, similar analyses can be readily carried out for MSW resonant flavour conversion, multi-generational mixing, spin precession in a magnetic field, neutrino decay. We hope to return to these issues in subsequent work.

The mass splitting Δ that can be searched for via supernova neutrinos is, indeed, very tiny. The energy and length scales associated with supernova neutrinos provide a unique window for very small mass splittings – a point noted earlier in ref. [18]. It has also been speculated that oscillation of neutrinos from active galactic nuclei or gamma ray bursts will also be sensitive to such small Δ [19]. Thus, for supernova neutrinos these variables allow us to probe very small values of Δ.

Acknowledgements

This work is supported by Eastern Centre for Research in Astrophysics, India.

References

[1] The super-Kamiokande collaboration: Y Fukuda *et al*, *Phys. Rev. Lett.* **81**, 1562 (1998)
T Kajita, talk at *Neutrino 1998*, (Takayama, Japan, 1998)
[2] Y Totsuka, super-Kamiokande (Univ. of Tokyo, 1990) Report No. ICRR-227-90-20
[3] Super-Kamiokande Collaboration: e-print hep-ex/9812011
[4] Sudbury Neutrino Observatory Proposal, Report No. SNO-87-12 (1987)
[5] J N Bahcall, *Neutrino Astrophysics* (Cambridge University Press, 1989)
[6] A preliminary account has been presented in Debasish Majumdar and Amitava Raychaudhuri, hep-ph/9812249, *Pramana – J. Phys.* **52**, L529–L536 (1999)
[7] J N Bahcall and E Lisi, *Phys. Rev.* **D54**, 5417 (1996)
[8] S M Bilenky and C Giunti, *Phys. Lett.* **B311**, 179 (1993); *ibid.* **B320**, 323 (1994)
G Fiorentini, M Lissia, G Mezzorani, M Moretti and D Vignaud, *Phys. Rev.* **D49**, 6298 (1994)
W Kwong and S P Rosen, *ibid.* **D51**, 6159 (1995)
[9] Srubabati Goswami, Debasish Majumdar and Amitava Raychaudhuri (work in progress)
[10] Debasish Majumdar, Kamales Kar, Alak Ray, Amitava Raychaudhuri and Firoza K Sutaria, e-print astro-ph/9807100 (submitted for publication)
[11] Georg G Raffelt, *Stars as Laboratories for Fundamental Physics* (The University of Chicago Press, 1996)
[12] A S Burrows, in *Supernova* edited by A G Petschek (Springer-Verlag, 1990)
A more detailed exposition of neutrino–deuteron interactions can be found in J N Bahcall, K Kubodera, and S Nozawa, *Phys. Rev.* **D38**, 1030 (1988)
[13] T Totani, K Sato, H E Dalhead and J R Wilson, *Astrophys. J.* **496**, 216 (1998)
[14] For a discussion of the effect of oscillations on the signal at SK and SNO see, for example, Sandhya Choubey, Debasish Majumdar and Kamales Kar, hep-ph/9809424, *J. Phys.* **G25**, 1001 (1999)

[15] Debasish Majumdar and Amitava Raychaudhuri, hep-ph/9901401, *Phys. Rev.* **D60**, 053001 (1999)
[16] F K Sutaria and A Ray, *Phys. Rev. Lett.* **79**, 1599 (1997)
[17] F K Sutaria, Ph.D. dissertation, University of Mumbai (Mumbai, India, 1997)
[18] P Reinartz and L Stodolsky, *Z. Phys.* **27**, 507 (1985)
[19] F Halzen and D Saltzberg, *Phys. Rev. Lett.* **81**, 4305 (1998)